



Exploring nucleic acid condensation and release from individual parvovirus particles with different physicochemical cues

K. Strobl^a, M.G. Mateu^b, Pedro J. de Pablo^{a,c,*}

^a Department of Condensed Matter Physics Universidad Autónoma de Madrid, 28049, Madrid, Spain

^b Centro de Biología Molecular Severo Ochoa (CSIC-UAM), Universidad Autónoma de Madrid, 28049, Madrid, Spain

^c Instituto de Física de la Materia Condensada (IFIMAC) Universidad Autónoma de Madrid, 28049, Madrid, Spain

ARTICLE INFO

Keywords:

ssDNA uncoating
Virus unpacking
Virus mechanics
Atomic force microscopy
Physical virology

ABSTRACT

In the infection cycle, viruses release their genome in the host cell during uncoating. Here we use a variety of physicochemical procedures to induce and monitor the in vitro uncoating of ssDNA from individual Minute Virus of Mice (MVM) particles. Our experiments revealed two pathways of genome release: i) filamentous ssDNA appearing around intact virus particles when using gradual mechanical fatigue and heating at moderate temperature (50 °C). ii) thick structures of condensed ssDNA appearing when the virus particle is disrupted by mechanical nanoindentations, denaturing agent guanidinium chloride and high temperature (70 °C). We propose that in the case of filamentous ssDNA, when the capsid integrity is conserved, the genome is externalized through one channel of the capsid pores. However, the disruption of virus particles revealed a native structure of condensed genome. The mechanical analysis of intact particles after DNA strands ejection confirm the stabilization role of ssDNA in MVM.

1. Introduction

The main functions of virus capsids are the protection, transport and delivery of the genetic material they enclose. For fulfilling these functions, they must be robust enough to protect the viral genome against aggression by external physicochemical factors. However, they also need to be sufficiently unstable to release their genome in the host cell for replication in the cytosol, on cytoplasmic membranes or in the nucleus (Yamauchi and Greber, 2016). During virus entry capsid shells are primed to disassemble in a thoroughly programmed manner. Uncoating of the viral genome may involve either partial or total disassembly of the capsid, or exit of the nucleic acid through a channel in the capsid. Uncoating is triggered by cellular factors that include mechanical strokes, binding to host cell receptors, enzymes and/or changes in pH or ion concentration (Flint et al., 2004; Greber and Fassati, 2003; Kilcher and Mercer, 2015).

Here we study the uncoating of the parvovirus Minute Virus of Mice (MVM), one of the smallest (~25 nm in diameter) and structurally simplest viruses (Cotmore and Tattersall, 2014). The MVM virion consists of an icosahedral capsid assembled from 60 equivalent protein subunits forming 20 trimeric building blocks (Llamas-Saiz et al., 1997; Reguera et al., 2005; Rioloobos et al., 2006). The capsid has spicules or

protrusions centered on the three-fold symmetry (S3) axes and pores channels formed by cylindrical structures on the five-fold (S5) axes, through which the single-stranded DNA (ssDNA) genome is released, and annular depressions in the two-fold (S2) axes between cylinders and spicules (Agbandje-McKenna et al., 1998; Llamas-Saiz et al., 1997). Its ~5kbp genome is packed inside without showing particular order (Agbandje et al., 1995), except for some segments that are anchored to wedges at the inner wall of the capsid, closer to the two-fold symmetry axes (Kontou et al., 2005). These segments, which account for 22% of the total genome (Agbandje-McKenna et al., 1998), exhibit atomic ordered structures and contribute to strengthen the virion by increasing both thermal stability (Reguera et al., 2005) and mechanical stiffness of the capsid regions close to the DNA anchor spots (Carrasco et al., 2006, 2008). However, the regions around the pores in the S5 symmetry axes remain free from bound DNA segments and, thus, mechanically flexible enough to facilitate the release of the genome through these channels (Castellanos et al., 2012). The pore cavity is 0.8 nm wide at equilibrium (Cotmore et al., 2010), but highly dynamic (van de Waterbeemd et al., 2017) to allow the translocation of the ssDNA molecule into a preformed capsid during packaging, and its extrusion during uncoating without capsid disassembly. The genome is released in the 3' to 5' direction, and the 5'-end may remain attached to the capsid interior wall (Cotmore

* Corresponding author. Department of Condensed Matter Physics Universidad Autónoma de Madrid, 28049 Madrid, Spain.

E-mail address: p.j.depablo@uam.es (P.J. de Pablo).

<https://doi.org/10.1016/j.virol.2023.01.010>

Received 1 November 2022; Accepted 12 January 2023

Available online 14 February 2023

0042-6822/© 2023 Published by Elsevier Inc.

et al., 2010).

In this work we use Atomic Force Microscopy (AFM) to induce and monitor ssDNA release from individual MVM virions. AFM has already applied to study the genome uncoating of human adenovirus (Martín-González et al., 2019; Ortega-Esteban et al., 2015) and T7 bacteriophage (Kellermayer et al., 2018). Here we use multiple physicochemical approaches for inducing viral DNA uncoating. They involve mechanical cues (nanoindentation or mechanical fatigue), a chemical agent (guanidinium chloride, GuHCl) or heating to 50 °C–70 °C.

2. Materials and methods

Virion production and purification. MVM virions were obtained from infected cells and purified as previously described (Carrasco et al., 2006).

AFM sample preparation. 20 µl of poly-L-lysine are pipetted onto the freshly cleaved mica and rinsed three times with 30 µl purified MQ-water after 15min incubation time. The surface is dried with nitrogen gas and then 20 µl of glutaraldehyde are pipetted. After 15min of incubation, the surface is again rinsed three times with 30 µl purified MQ-water and then dried with N₂ gas. 30 µl of the 1:10 dilution (mother MVM solution of 1 mg/ml) is pipetted onto the functionalized substrate and incubated for 30min, then rinsed three times with PBS (Phosphate Buffer Saline) without letting dry.

AFM is operated in liquid. A sharp tip located at the end of a microcantilever scans the virus particles adsorbed on the solid substrate (de Pablo, 2019) by using jumping mode. In this mode the cantilever approaches to the sample until a certain bending force is achieved to obtain the height value of the topography pixel. Afterwards the cantilever is retracted to release the tip-sample contact and move to the next pixel (Ortega-Esteban et al., 2012). We used OML-RC800PSA and PNP-DB-50 cantilevers that were routinely calibrated with the Sader's method (Sader et al., 1999).

Correlative fluorescence images were obtained in total internal reflection microscopy (TIRFM) mounted with the AFM (Strobl et al., 2022) by using a blue laser (488nm wavelength) to excite RiboGreen® fluorophore (ThermoFisher), which is used as a ssDNA reporter (Ortega-Esteban et al., 2015).

3. Results

MVM virions adsorbed on mica were imaged as round particles (Fig. 1A), and the resolution achieved was enough to reveal the five trimers and the pore structure centered around a S5 axis (Fig. 1B). The

average measured virion height was 26.5 nm (Fig. 1C), just below its expected diameter ~28 nm (Cotmore and Tattersall, 2014). This small difference may rely on a slight deformation (~5%), probably due to the interaction between the virus particles and the surface (Zeng et al., 2017). The integrity of the virus particles was tested by correlative AFM-fluorescence microscopy (Strobl et al., 2022). MVM virus particles were coadsorbed with fluorescence Tetraspeck® beads of 100 nm of diameter (T7279 ThermoFisher), in the presence of a molecular reporter of ssDNA (RiboGreen®). The red square in Fig. 1D encloses three fluorescence beads (circled) and a wide bright spot. The simultaneous AFM image (Fig. 1E) shows the same three beads (circled) and many virus particles (pink) which are not seen in the fluorescence image. AFM data revealed that the wide bright spot (Fig. 1E, square) corresponds to a large patch of DNA attached on the surface which emits fluorescence when bound to RiboGreen® (Fig. 1F, yellow). These observations suggest that most virus particles are intact, with its nucleic acid still fully shielded from the exterior, because they were visible in AFM images (Fig. 1E), but did not emit fluorescence (Fig. 1D), indicating that RiboGreen® molecules did not interact with the viral nucleic acid inside the particle.

3.1. Genome externalization by nanoindentation

The AFM cantilever is a force transducer which can be used to achieve a gradual, controlled deformation of a virus particle in order to quantify its mechanical properties (de Pablo, 2019). Once a MVM virion was selected (Fig. 2A), the tip was approached to the apex of the particle at constant speed (100 nm/s). After the tip established contact with the capsid, the bending force increased gradually as the virus particle was being linearly deformed (Fig. 2B). From this linear deformation it is possible to derive the stiffness of the particle (~0.5 N/m). A step in the force versus deformation curve was observed at 2.1 nN, which was associated to breakage of the viral particle (de Pablo, 2019). After the nonlinear event, AFM imaging (Fig. 2C) revealed a reduction of 5 nm in the height of the particle (Fig. 2D) which showed that it had actually been fractured. In addition, patches of condensed material were observed around the fractured virus particles. The height of this material is compatible with the thickness of a ssDNA molecule, as determined by AFM (Moreno-Herrero et al., 2003).

3.2. Genome externalization by inducing mechanical fatigue

AFM imaging in jumping mode implies applying thousands of indentations at low force (Martín-González et al., 2021). Therefore, mere

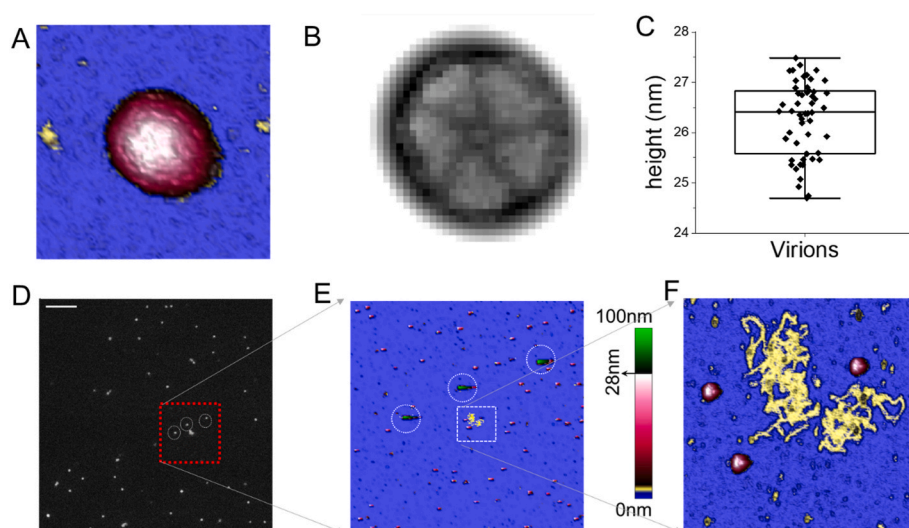


Fig. 1. Topography characterization of MVM virus particles. A) MVM virus particle. Image size 200 nm × 200 nm. B) Filtered AFM topography data showing the 5-fold symmetry axis (100 nm × 100 nm). C) Box plot of virus particles diameter. D) Fluorescence image. Tetraspeck beads are circled. Scale bar 6 µm. The AFM data of the red square (E) shows three beads of (D). White square is zoomed in (F), showing three intact MVM particles (pink) and the DNA patch (yellow). Image size 1 µm × 1 µm.

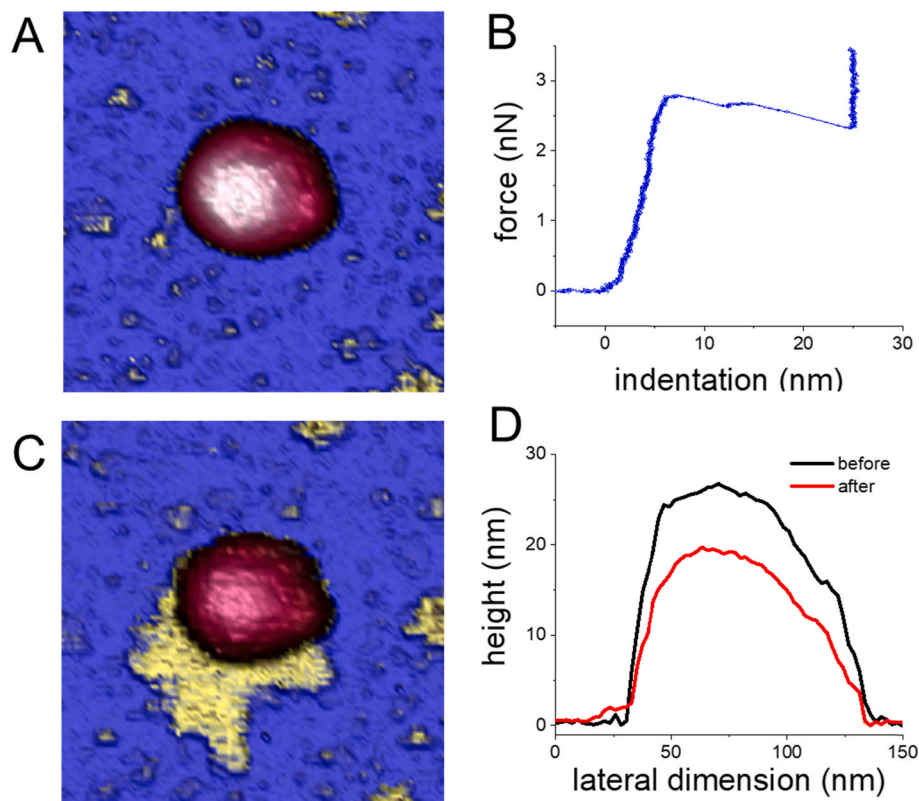


Fig. 2. Genome externalization with nano-indentation. A) shows an intact MVM virion. Image size of 250 nm \times 250 nm. B) presents the nano-indentation of the AFM tip, showing the linear deformation of the particle from 0 to 6 nm. At 2.8 nN the particle breaks and the tip reaches the solid substrate. C) AFM image of the particle after nano-indentation, showing a lower capsid and a patch of genome (yellow). Same image size than (A). D) Profiles of the virus particle before (black) and after (red) the nanoindentation of (B).

imaging of viruses is already applying periodic cycles of force at ~ 100 pN all over the virus particle extension during one image. If the same virus is consecutively imaged, it is subjected to mechanical fatigue (Schijve, 2001) and this can promote gradual disassembly and genome

externalization (Ortega-Esteban et al., 2013). Material fatigue was induced in MVM virions by AFM imaging (Fig. 3A). After a high enough number of cycles, long and thin filaments whose height approximately corresponds to the thickness of a ssDNA molecule were observed around

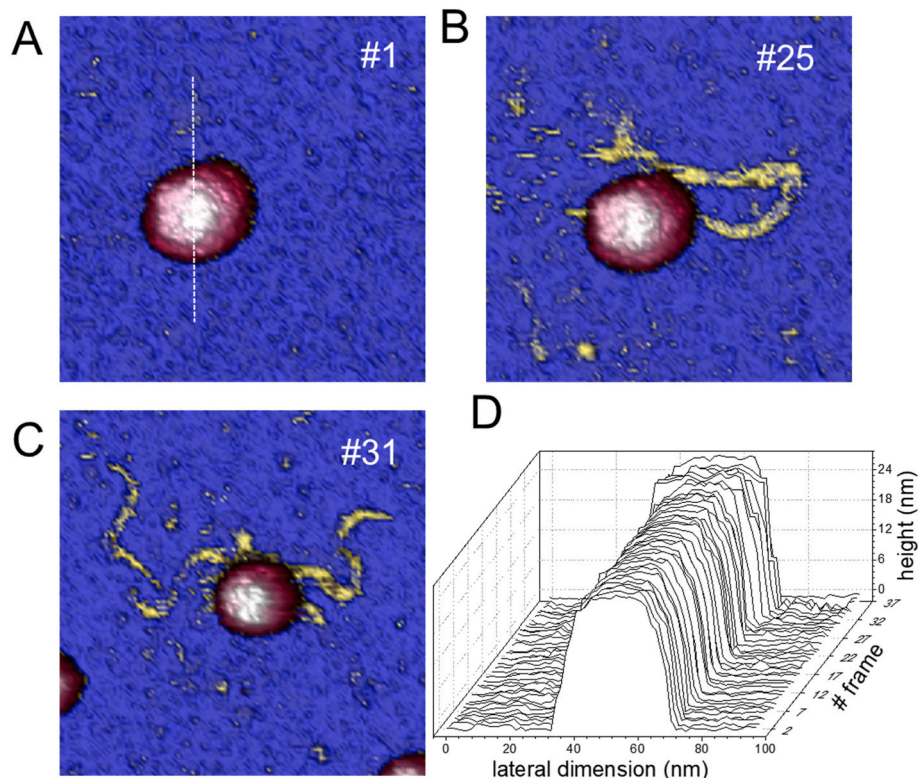


Fig. 3. Genome externalization with mechanical fatigue at 100 pN. A), B) and C) AFM topographies of a MVM virus particles after 1, 25 and 31 consecutive frames, respectively. Image size is 200 nm \times 200 nm for A) and B), and 300 nm \times 300 nm for C). B) and C) micrographs show the externalization of the viral genome in the form of filament (yellow). D) Topographical profiles obtained along the white dashed line of (A) in all the frames, showing a constant height which indicates that the capsid remains intact along the process. Supplementary movie SMV1 shows the 36 frames where the mechanical fatigue extracts the genome.

the imaged particle (Fig. 3B and C). The ssDNA molecule was ejected from the fatigued virus particle without any detectable alteration in height or morphology (Fig. 3D) which indicates that no capsid subunits had been lost.

3.3. Genome externalization by treatment with GuHCl

GuHCl is a protein denaturing agent (Zarrine-Afsar et al., 2006) that has been used before for destabilizing virus particles (Snijder et al., 2017). First, MVM virus particles were visualized by AFM in order to verify that the adsorbed particles were of undamaged. Then, the incubated sample was rinsed multiple times with 4 M GuHCl. Due to its high viscosity, it was important to ensure complete fluid exchange. After this treatment, many adsorbed virions were still assembled (Fig. 4A). However, some viral particles were disrupted due to mechanical stress when they were imaged at low force (Fig. 4B). Extra material was observed around the disrupted particles, which most likely correspond to patches of condensed nucleic acid weakly bound to the surface (Fig. 4B and C).

3.4. Genome externalization by heating

Temperature is a physical parameter that is often used to induce virus uncoating. In human adenovirus, heating virus particles to 40 °C–50 °C promotes the release of capsomers and the disruption of the capsid (Pérez-Berná et al., 2012). The ssDNA of MVM is released without capsid disassembly at moderate temperatures, and the capsid is disrupted at ~70 °C or higher temperatures (Ros et al., 2006).

The temperature of MVM virus particles in the test tube was raised during 15 min prior to incubation on the mica surface. The exposure of virions to temperatures in the range of 50 °C resulted in genome release without capsid disassembly (Fig. 5A). Although virions ejected large

amounts of DNA, the height of the capsid remained on its nominal value of 26 nm (Fig. 5C, black). It is remarkable that the expelled DNA remained bound to the capsid, and filaments about 2–3 nm in diameter were observed. The externalized ssDNA accounts for almost 90% of the total MVM genome. Increasing the temperature to 70 °C in the test tube resulted in catastrophic consequences for the virions. Capsids appear completely disrupted and only a few fragments of DNA are visible.

As an alternative approach, the adsorbed virions were directly heated to 70 °C. This treatment resulted in partially destroyed virus particles that were surrounded by patches of condensed DNA (Fig. 5B). Virus particles so disrupted hardly reached a height of 10 nm (Fig. 5C, red).

3.5. Changes in the mechanical properties of the MVM particle upon genome uncoating

In order to elucidate the interplay between uncoating mechanisms and the mechanical properties of the capsid, nanoindentations were performed on virions that exposed genetic material after fatigue and heating experiments where the size of the virus particle was conserved. In this way we aimed to explore the effects of the genome absence on the stiffness and breaking force of intact viruses. Fig. 6 shows that virus particles changed both their stiffness (Fig. 6A) and breaking force (Fig. 6B) after ejecting their genome. Their stiffness dropped from ~0.55 N/m to ~0.42 N/m and ~0.37 N/m for fatigue and heat experiments, respectively. The breaking force decreased from ~2.2 nN to ~1.8 nN and ~1.7 nN for fatigue and heat procedures, respectively. Fatigue and heat have similar effects on stiffness and breaking force values that are practically indistinguishable.

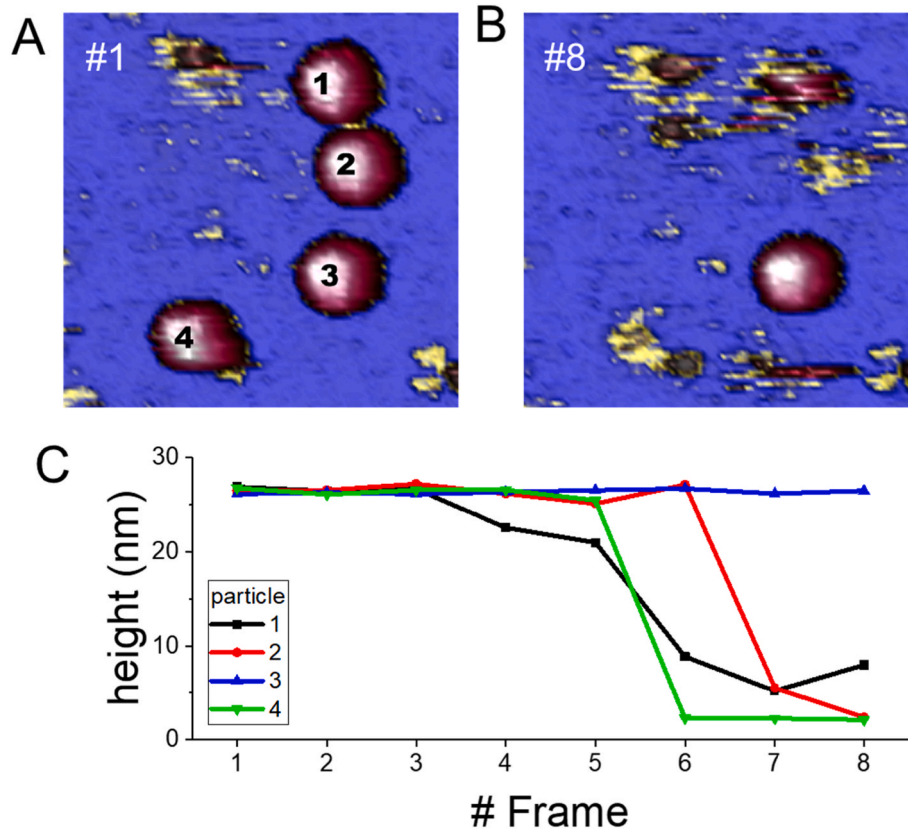


Fig. 4. Genome externalization with GuHCl 4M. A) AFM image of the first frame showing 4 intact virus particles. B) AFM topography after 7 consecutive frames, showing the destruction of particles 1, 2 and 4, leaving some debris on the surface. C) Height evolution showing the integrity of each labeled particle of panel (A). Only particle 3 survives after the mechanical fatigue process. Images size is 400 nm × 400 nm. Supplementary movie SMV2 shows the complete process.

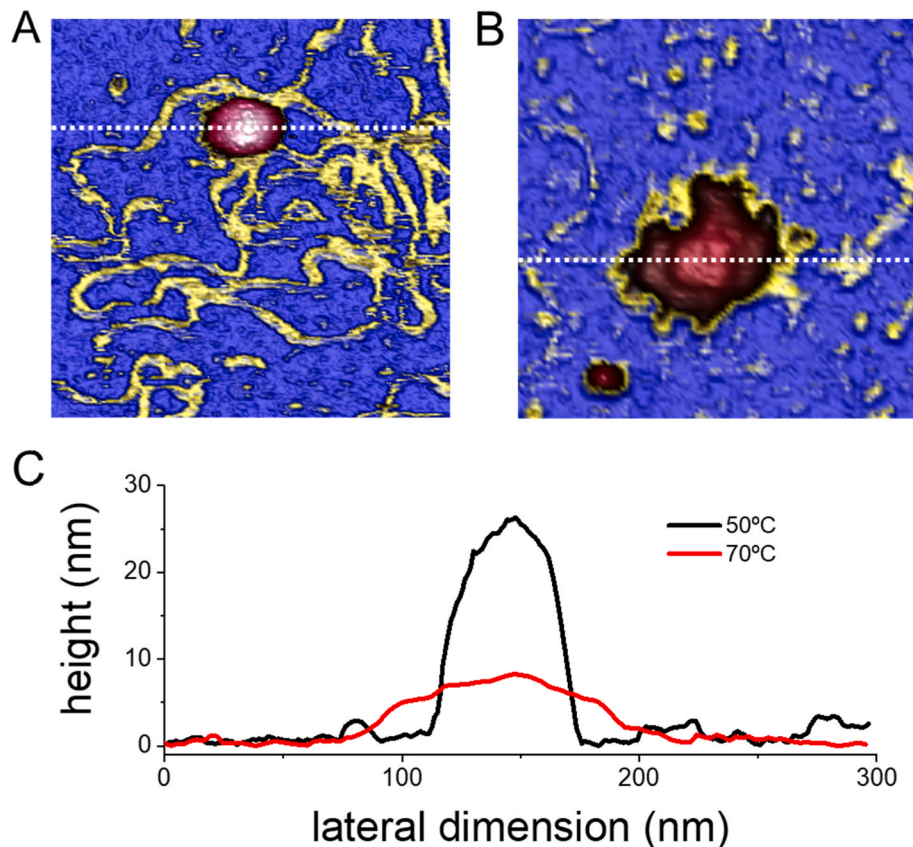


Fig. 5. Genome externalization with temperature. A) AFM image of a virion heated at 50 °C during 5 min, showing the capsid (pink) and the ejected genome (yellow). B) AFM image of a virion heated at 70 °C during 5 min. C) Topography profiles of both particles obtained at the white dotted lines of (A) and (B).

4. Discussion

Our study shows that when the virus particle is broken by nano-indentations reaching ~ 2 nN, GuHCl treatment at 4 M, and high temperature (70 °C), a densely condensed patch of genome was externalized and captured on the surface. This fact indicates that there are interactions between secondary and tertiary ssDNA structures that induce the condensation of the viral genome inside the virus cavity. This condensation remains when the capsid is quickly disrupted, without time for disentangling the ssDNA filaments. The sudden capsid disruption seem to dissociate the ssDNA-capsid interactions through the wedges of nucleic acids that are regularly inserted in cavities of the capsid lumen (Carrasco et al., 2006). Hence, the externalization of condensed genome is related to the integrity loss of the virus particle. The broken protein shell is not able to keep the ssDNA inside, so that it escapes outside revealing the compact, native form in which it is packaged inside the capsid. ssDNA is strongly reactive and tends to fold acquiring secondary and tertiary structures. This fact is evinced by the height of the externalized genomic condensates, that was always bigger than 2 nm.

The externalization of ssDNA in filaments was observed in fatigue experiments and in thermal treatment of virions at 50 °C. In both approaches the virus particles keep their size (Figs. 3 and 6) and apparently, did not loose any capsomer. These results are compatible with the hypothesis of the physiological uncoating of MVM virions: it is suggested that the ssDNA leaves the virus particle through one of the capsid pores, without any disassembly process implying its structural disruption (Ros et al., 2006). In fact, the thermal ssDNA externalization parallelizes the experiments performed with bulk techniques (Ros et al., 2006), but using a single molecule nanotechnology approach. ssDNA should be disentangled before leaving the capsid through the channel. Therefore,

both mechanical fatigue and mild heat experiments provide enough energy to cease DNA-capsid interaction and disrupt tertiary and secondary ssDNA structures, thus allowing the ssDNA diffusion through a single pore of the capsid.

The mechanical evolution of stiffness (Fig. 6A) and breaking force (Fig. 6B) is compatible with the reinforcing role of ssDNA wedges inserted in the lumen of the capsid (Carrasco et al., 2006). Since fatigued and heated virus particles ejected between 40% and 80% of their genome but kept their structural integrity, it is likely to consider that some wedges of ssDNA left their cavities and stopped the mechanical reinforcement of the capsid (Fig. 6).

The ssDNA externalization due to chaotropic agent GuHCl 4 M vulnerated viral stability against mechanical fatigue. As GuHCl disrupts hydrogen bonding leading to protein unfolding and dsDNA unzipping, it should not affect ssDNA in its primary structure. Therefore, we expected to observe uncoiled ssDNA fragments bound to the surface, but there were only molten-like patches at the locations where virions were initially adsorbed. These could correspond to the capsid proteins denatured to random coils. Nevertheless, GuHCl is widely used for DNA isolation (Pramanick et al., 1976), suggesting that the genome kept bound to the denatured proteins by an unknown mechanism that surely is not based on hydrogen bonding. These complexes could not be imaged properly by AFM because they were not fully fixed to the substrate (Fig. 4B).

Our work states that in vitro, MVM virus particles need energy to induce ssDNA uncoating in a filamentous state through the pore, such as fatigue or moderate heat. It remains as an open question to know the responsible mechanism triggering ssDNA externalization in vivo.

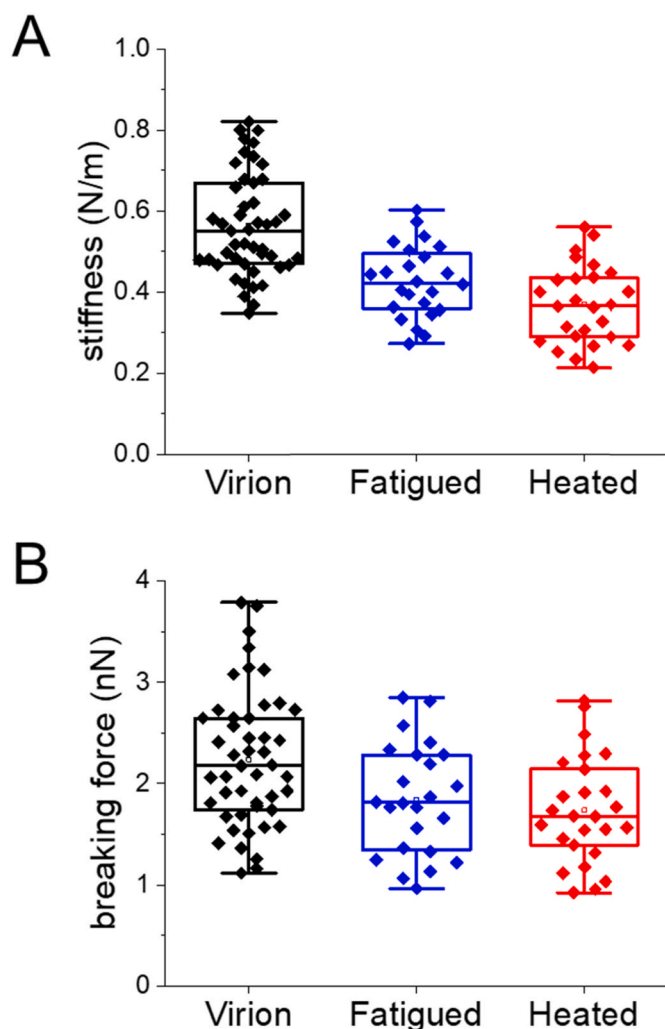


Fig. 6. Mechanical evolution of intact particles upon genome externalization. A) Stiffness or spring constant charts for intact (black), mechanical fatigued (blue) and heated (red) capsids. B) Breaking force charts for intact (black), mechanical fatigued (blue) and heated (red) capsids.

Declaration of competing interest

The authors declare that they have no known competing financial interests or personal relationships that could have appeared to influence the work reported in this paper.

Acknowledgements

P.J.d.P. acknowledges support by grants received from the Spanish Ministry of Economy, Industry and Competitiveness projects (FIS2017-89549-R, FIS2017-90701-REDT and PID2021-126608OB-I00) and the Human Frontiers Science Program (HFSPO RGP0012/2018). M.G.M. acknowledges Alicia Rodríguez-Huete for technical assistance and support by grant PID2021-126973OB-I00 and an institutional grant from the Ramón Areces Foundation. M.G.M. is an associate member of the Institute for the Physics of Complex Systems, Zaragoza, Spain.

Appendix A. Supplementary data

Supplementary data to this article can be found online at <https://doi.org/10.1016/j.virol.2023.01.010>.

References

- Agbandje, M., Parrish*, C.R., Rossmann, M.G., 1995. The structure of parvoviruses. *Semin. Virol.* 6, 299–309. <https://doi.org/10.1006/smvy.1995.0036>.
- Agbandje-McKenna, M., Llamas-Saiz, A.L., Wang, F., Tattersall, P., Rossmann, M.G., 1998. Functional implications of the structure of the murine parvovirus, minute virus of mice. *Structure* 6, 1369–1381. [https://doi.org/10.1016/s0969-2126\(98\)00137-3](https://doi.org/10.1016/s0969-2126(98)00137-3).
- Carrasco, C., Carreira, A., Schaap, I.A.T., Serena, P.A., Gómez-Herrero, J., Mateu, M.G., Pablo, P.J. de, 2006. DNA-mediated anisotropic mechanical reinforcement of a virus. *Proc. Natl. Acad. Sci. USA* 103, 13706–13711. <https://doi.org/10.1073/pnas.0601881103>.
- Carrasco, C., Castellanos, M., Pablo, P.J. de, Mateu, M.G., 2008. Manipulation of the mechanical properties of a virus by protein engineering. *Proc. Natl. Acad. Sci. USA* 105, 4150–4155. <https://doi.org/10.1073/pnas.0708017105>.
- Castellanos, M., Pérez, R., Carrasco, C., Hernando-Pérez, M., Gómez-Herrero, J., De Pablo, P.J., Mateu, M.G., 2012. Mechanical elasticity as a physical signature of conformational dynamics in a virus particle. *Proc. Natl. Acad. Sci. U. S. A.* 109, 12028–12033. <https://doi.org/10.1073/pnas.1207437109>.
- Cotmore, S.F., Tattersall, P., 2014. Parvoviruses: small does not mean simple. *Annual Review of Virology* 1, 517–537. <https://doi.org/10.1146/annurev-virology-031413-085444>.
- Cotmore, S.F., Hafenstein, S., Tattersall, P., 2010. Depletion of virion-associated divalent cations induces parvovirus minute virus of mice to eject its genome in a 3'-to-5' direction from an otherwise intact viral particle. *J. Virol.* 84, 1945–1956. <https://doi.org/10.1128/JVI.01563-09>.
- de Pablo, P.J., 2019. The application of atomic force microscopy for viruses and protein shells: imaging and spectroscopy. *Adv. Virus Res.* 105, 161–187.
- Flint, S.J., Enquist, L.W., Racaniello, V.R., Skalka, A.M., 2004. *Principles of Virology*. ASM Press, Washington D.C.
- Greber, U.F., Fassati, A., 2003. Nuclear import of viral DNA genomes. *Traffic* 4, 136–143. <https://doi.org/10.1034/j.1600-0854.2003.00114.x>.
- Kellermayer, M.S.Z., Vörös, Z., Csik, G., Herényi, L., 2018. Forced phage uncorking: viral DNA ejection triggered by a mechanically sensitive switch. *Nanoscale* 10, 1898–1904. <https://doi.org/10.1039/c7nr05897g>.
- Kilcher, S., Mercer, J., 2015. DNA virus uncorking. *Virology*, 60th Anniversary Issue 479–480, 578–590. <https://doi.org/10.1016/j.virol.2015.01.024>.
- Kontou, M., Govindasamy, L., Nam, H.-J., Bryant, N., Llamas-Saiz, A.L., Foces-Foces, C., Hernando, E., Rubio, M.-P., McKenna, R., Almendral, J.M., Agbandje-McKenna, M., 2005. Structural determinants of tissue tropism and in vivo pathogenicity for the parvovirus minute virus of mice. *J. Virol.* 79, 10931–10943. <https://doi.org/10.1128/JVI.79.17.10931-10943.2005>.
- Llamas-Saiz, A.L., Agbandje-McKenna, M., Wikoff, W.R., Bratton, J., Tattersall, P., Rossmann, M.G., 1997. Structure determination of minute virus of mice. *Acta Crystallogr. D* 53, 93–102. <https://doi.org/10.1107/S0907444996010566>.
- Martín-González, N., Hernando-Pérez, M., Condezo, G.N., Pérez-Illana, M., Süber, A., Reguera, D., Ostapchuk, P., Hearing, P., San Martín, C., de Pablo, P.J., 2019. Adenovirus major core protein condenses DNA in clusters and bundles, modulating genome release and capsid internal pressure. *Nucleic Acids Res.* 47, 9231–9242.
- Martín-González, N., Ibáñez-Freire, P., Ortega-Esteban, Á., Laguna-Castro, M., San Martín, C., Valbuena, A., Delgado-Buscalioni, R., de Pablo, P.J., 2021. Long-range cooperative disassembly and aging during adenovirus uncoating. *Phys. Rev. X* 11, 021025. <https://doi.org/10.1103/PhysRevX.11.021025>.
- Moreno-Herrero, F., Colchero, J., Baró, A.M., 2003. DNA height in scanning force microscopy. *Ultramicroscopy* 96, 167–174. [https://doi.org/10.1016/S0304-3991\(03\)00004-4](https://doi.org/10.1016/S0304-3991(03)00004-4).
- Ortega-Esteban, A., Horcas, I., Hernando-Pérez, M., Ares, P., Pérez-Berná, A.J., San Martín, C., Carrascosa, J.L., de Pablo, P.J., Gómez-Herrero, J., 2012. Minimizing tip-sample forces in jumping mode atomic force microscopy in liquid. *Ultramicroscopy* 114, 56–61. <https://doi.org/10.1016/j.ultramic.2012.01.007>.
- Ortega-Esteban, A., Pérez-Berná, A.J., Menéndez-Conejero, R., Flint, S.J., Martín, C.S., de Pablo, P.J., 2013. Monitoring dynamics of human adenovirus disassembly induced by mechanical fatigue. *Sci. Rep.* 3, 1434. <https://doi.org/10.1038/srep01434>.
- Ortega-Esteban, A., Bodensiek, K., San Martín, C., Suomalainen, M., Greber, U.F., de Pablo, P.J., Schaap, I.A., 2015. Fluorescence tracking of genome release during mechanical unpacking of single viruses. *ACS Nano* 9, 10571–10579. <https://doi.org/10.1021/acsnano.5b03020>.
- Ortega-Esteban, A., Condezo, G.N., Pérez-Berná, A.J., Chillón, M., Flint, S.J., Reguera, D., San Martín, C., De Pablo, P.J., 2015. Mechanics of viral chromatin reveals the pressurization of human adenovirus. *ACS Nano* 9, 10826–10833.
- Pérez-Berná, A.J., Ortega-Esteban, A., Menéndez-Conejero, R., Winkler, D.C., Menéndez, M., Steven, A.C., Flint, S.J., de Pablo, P.J., San Martín, C., 2012. The role of capsid maturation on adenovirus priming for sequential uncoating. *J. Biol. Chem.* 287, 31582–31595. <https://doi.org/10.1074/jbc.M112.389957>.
- Pramanick, D., Forstová, J., Pivec, L., 1976. 4 M guanidine hydrochloride applied to the isolation of DNA from different sources. *FEBS Lett.* 62, 81–84. [https://doi.org/10.1016/0014-5793\(76\)80021-x](https://doi.org/10.1016/0014-5793(76)80021-x).
- Reguera, J., Grueso, E., Carreira, A., Sánchez-Martínez, C., Almendral, J.M., Mateu, M.G., 2005. Functional relevance of amino acid residues involved in interactions with ordered nucleic acid in a spherical virus. *J. Biol. Chem.* 280, 17969–17977. <https://doi.org/10.1074/jbc.M500867200>.
- Riolobos, L., Reguera, J., Mateu, M.G., Almendral, J.M., 2006. Nuclear transport of trimeric assembly intermediates exerts a morphogenetic control on the icosahedral parvovirus capsid. *J. Mol. Biol.* 357, 1026–1038. <https://doi.org/10.1016/j.jmb.2006.01.019>.

- Ros, C., Baltzer, C., Mani, B., Kempf, C., 2006. Parvovirus uncoating in vitro reveals a mechanism of DNA release without capsid disassembly and striking differences in encapsidated DNA stability. *Virology* 345, 137–147. <https://doi.org/10.1016/j.virol.2005.09.030>.
- Sader, J.E., Chon, J.W.M., Mulvaney, P., 1999. Calibration of rectangular atomic force microscope cantilevers. *Rev. Sci. Instrum.* 70, 3967–3969.
- Schijve, Jaap, 2001. *Fatigue of Structures and Materials*. Kluwer Academic Publishers, Dordrecht.
- Snijder, J., Radtke, K., Anderson, F., Scholtes, L., Corradini, E., Baines, J., Heck, A.J.R., Wuite, G.J.L., Sodeik, B., Roos, W.H., 2017. Vertex-Specific proteins pUL17 and pUL25 mechanically reinforce herpes simplex virus capsids. *J. Virol.* 91 <https://doi.org/10.1128/JVI.00123-17>.
- Strobl, K., Selivanovitch, E., Ibáñez-Freire, P., Moreno-Madrid, F., Schaap, I.A.T., Delgado-Buscalioni, R., Douglas, T., de Pablo, P.J., 2022. Electromechanical photophysics of GFP packed inside viral protein cages probed by force-fluorescence hybrid single-molecule microscopy. *Small* 18, 2200059. <https://doi.org/10.1002/smll.202200059>.
- van de Waterbeemd, M., Llauro, A., Snijder, J., Valbuena, A., Rodríguez-Huete, A., Fuertes, M.A., de Pablo, Pedro, J., Mateu, M.G., Heck, A.J.R., 2017. Structural analysis of a temperature-induced transition in a viral capsid probed by HDX-MS. *Biophys. J.* 112, 1157–1165. <https://doi.org/10.1016/j.bpj.2017.02.003>.
- Yamauchi, Y., Greber, U.F., 2016. Principles of virus uncoating: cues and the snooker ball. *Traffic* 17, 569–592. <https://doi.org/10.1111/tra.12387>.
- Zarrine-Afsar, A., Mittermaier, A., Kay, L.E., Davidson, A.R., 2006. Protein stabilization by specific binding of guanidinium to a functional arginine-binding surface on an SH3 domain. *Protein Sci.* 15, 162–170. <https://doi.org/10.1110/ps.051829106>.
- Zeng, C., Hernando-Perez, M., Dragnea, B., Ma, X., van der Schoot, P., Zandi, R., 2017. Contact mechanics of a small icosahedral virus. *Phys. Rev. Lett.* 119, 038102 <https://doi.org/10.1103/PhysRevLett.119.038102>.